Available online at www.sciencedirect.com
SCIENCE DIRECT®
Biochemical Pharmacology 65 (2003) 1931–1942
Biochemical Pharmacology
www.elsevier.com/locate/biochempharm

Expression of the murine CB_2 cannabinoid receptor using a recombinant Semliki Forest virus

John M. Olson[a], Suzanne J. Kennedy[b], Guy A. Cabral[b,*]

[a]*Department of Biological Chemistry, UCLA School of Medicine, Los Angeles, CA 90095-1737, USA*
[b]*Department of Microbiology and Immunology, Virginia Commonwealth University, 1101 E. Marshall Street, Richmond, VA 23298-0678, USA*

Received 5 June 2002; accepted 2 December 2002

Abstract

A recombinant Semliki Forest virus (SFV) RNA construct, SFV1-mCB_2 RNA, was employed for the high-level expression of the murine CB_2 (mCB_2) cannabinoid receptor in baby hamster kidney cells. Biosynthetic radiolabel incorporation studies in concert with urea-sodium dodecylsulfate–polyacrylamide gel electrophoresis (urea-SDS–PAGE) and western immunoblotting revealed that two major proteins of approximately 26 and 40 kDa were produced by the construct. The 40 kDa product, but not the 26 kDa product, was glycosylated as determined by 2-deoxy-D-glucose incorporation and peptide-*N*-glycosidase F digestion analysis. Assessment of [^{3}H]CP55940 ([^{3}H]-(−)-*cis*-3-[2-hydroxy-4-(1,1-dimethylheptyl)phenyl]-*trans*-4-(3-hydroxypropyl)cyclohexanol) binding data for membranes of cells transfected with SFV1-mCB_2 RNA indicated a K_d of 0.35 ± 0.04 nM and a B_{max} of 24.4 ± 2.7 pmol/mg. A rank order of binding affinities for cannabinoids, which paralleled that reported for native mCB_2 receptors, was observed. The CB_2 receptor-specific antagonist SR144528 (*N*-[(1*S*)-endo-1,3,3-trimethyl bicyclo[2.2.1]heptan-2-yl]-5-(4-chloro-3-methylphenyl)-1-(4-methylbenzyl)-pyrazole-3-carboxamide) blocked binding of [^{3}H]CP55940, while the CB_1 receptor-specific antagonist SR141716A [*N*-(piperidin-1-yl)-5-(4-chlorophenyl)-1-(2,4-dichlorophenyl)-4-methyl-1*H*-pyrazole-3-carboxamide hydrochloride] had a minimal effect. These results indicate that the recombinant receptor expressed from SFV1-mCB_2 RNA exhibits properties, including ligand binding features, that are consistent with those for the native mCB_2 receptor. However, the presence of both 26 and 40 kDa receptor species is consistent with alternative translation from two AUG start sites using the SFV1-mCB_2 RNA expression system.

Keywords: Cannabinoid receptor; CB_2 receptor; CB_2 receptor expression; CB_2 receptor protein; Murine CB_2 receptor; Semliki Forest virus CB_2 receptor construct

1. Introduction

Cannabinoids have been reported to modulate cellular functions by both receptor and non-receptor-mediated modes [1]. To date, two cannabinoid receptor types have been identified. The first of these, the CB_1, is found primarily in neural tissue [2,3] and testis [4], although it is also present at relatively low levels in cells of the immune system [5–7]. A second receptor, designated the CB_2, has been identified in cells of the immune system [7,8], in adult uterine tissue and embryonic organs [9], and in adult retina [10]. Both receptors are members of the seven-transmembrane domain family of receptors that couple to G proteins [3,4]. The CB_1 is highly conserved across mammalian species and shares greater than 97% identity for human, mouse, and rat. The CB_2, on the other hand, exhibits greater inter-species variability [8,11,12]. The human CB_2 was cloned originally from a human acute myeloid leukemia cell line (HL60) [8] using degenerate primers for G protein-coupled receptors and shares 68% homology with the CB_1 in the transmembrane domains but only 44% homology in overall protein sequence. A mouse

* Corresponding author. Tel.: +1-804-828-2306; fax: +1-804-828-8220.
E-mail address: gacabral@hsc.vcu.edu (G.A. Cabral).

Abbreviations: BHK, baby hamster kidney; CB_1, cannabinoid receptor type 1; CB_2, cannabinoid receptor type 2; FBS, fetal bovine serum; FITC, fluorescein-5-isothiocyanate; G_i, G inhibitory; G-MEM, Glasgow Minimum Essential Medium; IgG, immunoglobulin G; mCB_2, murine CB_2 receptor; PMSF, phenylmethylsulfonyl fluoride; PNGase F, peptide-*N*-glycosidase F; SFV, Semliki Forest virus; SSC, sodium chloride/sodium citrate; TBS, Tris-buffered saline; TCA, trichloroacetic acid; TSA, Tris/saline/azide; urea-SDS–PAGE, urea-sodium dodecylsulfate–polyacrylamide gel electrophoresis.

0006-2952/03/$ – see front matter © 2003 Elsevier Science Inc. All rights reserved.
doi:10.1016/S0006-2952(03)00200-4

CB_2 gene has been cloned using the human CB_2 cDNA as a probe for screening a murine spleen cDNA library and has been shown to possess 82% identity to the human CB_2 [11]. The murine CB_2 (mCB_2) protein, as extrapolated from its cDNA coding sequence, contains one potential glycosylation site in the extracellular domain and several potential phosphorylation sites at the C terminus. These include putative phosphorylation sites for protein kinase C, casein kinase II, and cyclic AMP-dependent protein kinase. Recently, Griffin *et al*. [12] cloned and characterized CB_2 from the rat. Analysis of its coding sequence indicates 90% nucleic acid identity between rat and mouse and 81% nucleic acid identity between rat and human.

Although a plethora of data has been accumulated concerning the functional relevance of the CB_1 receptor, there is a paucity of similar data for the CB_2. The preponderance of this receptor in cells of the immune system [6–8], and the numerous reports that cannabinoids alter the functional activities of immune cells [13–15], suggest that this receptor plays a role in immune regulation. Reports that CB_2 receptors are involved in the modulation of B-cell differentiation [16], are linked functionally to cannabinoid-mediated inhibition of processing of select antigens by macrophages [17], and are implicated in cannabinoid-mediated inhibition of anti-tumor activity [18] and *in vitro* migration of macrophages [19] are consistent with this postulate. However, few other studies have been conducted that have explored the functional relevance of CB_2 receptors as they relate to immune functional activities. Studies on CB_2 function, other than those utilizing pharmacological approaches, have been hampered by the relatively low numbers of these receptors on various immune cell subpopulations. Thus, strategies that would allow for high-level expression of the CB_2, particularly in the context of post-translational modification and cellular compartmentalization peculiar to distinctive mammalian cell types, would facilitate the investigation of the functional relevance of these receptors using biochemical and immunocytochemical approaches.

In the present investigation, we report on the application of a recombinant SFV expression system for high level production of the mCB_2 in mammalian cells. The SFV system, over traditional bacterial and baculovirus protein expression systems, allows for the expression of protein that is susceptible to post-translational modifications and cell membrane compartmentalization contextual to the host cell type. The recombinant mCB_2 which was expressed exhibited several biological and pharmacological properties, including immunospecificity and ligand binding, that are consistent with those determined for the native mCB_2. However, two major receptor protein species of approximately 26 and 40 kDa were produced, suggestive of translation from two AUG start sites from the CB_2 sequence in the recombinant SFV RNA genome.

2. Materials and methods

2.1. Reagents

Tissue culture reagents including Dulbecco's PBS were purchased from GIBCO-BRL, except for FBS, which was obtained from BioWhittaker. Restriction enzymes were obtained from New England Biolabs. Reagents for *in vitro* transcription were obtained from GIBCO-BRL. Aprotinin (5–10 trypsin inhibitor units), 2-deoxy-D-glucose, PNGase F, and 1,10-phenanthroline were purchased from the Sigma Chemical Co. Blocker Casein in TBS was purchased from the Pierce Chemical Co. Normal rabbit IgG and FITC-conjugated goat anti-rabbit IgG were purchased from Cappel. Aquamount was obtained from Lerner Laboratories. [^{3}H]CP55940 ([^{3}H]-(−)-*cis*-3-[2-hydroxy-4-(1,1-dimethylheptyl)phenyl]-*trans*-4-(3-hydroxypropyl)-cyclohexanol), CP55940, and WIN55212-2 [(*R*)-(+)-[2,3-dihydro-5-methyl-3-[4-morpholinylmethyl]pyrrolo[1,2,3-de]-1,4-benzoxazin-6-yl]-1-naphthalenylmethanone] were provided by Dr. Billy R. Martin (Department of Pharmacology and Toxicology, Virginia Commonwealth University). The CB_1 and CB_2 receptor antagonists SR141716A [*N*-(piperidin-1-yl)-5-(4-chlorophenyl)-1-(2,4-dichlorophenyl)-4-methyl-1*H*-pyrazole-3-carboxamide hydrochloride] and SR144528 (*N*-[(1*S*)-endo-1,3,3-trimethyl bicyclo[2.2.1]heptan-2-yl]-5-(4-chloro-3-methylphenyl)-1-(4-methylbenzyl)-pyrazole-3-carboxamide), respectively, were provided by Sanofi Recherche.

2.2. Cell culture

Baby hamster kidney (BHK-21) cells (ATCC No. CCL-10) were cultured in G-MEM with 2 mM glutamine, 10% tryptose phosphate broth, 10 mM HEPES (pH 7.3), 100 U/mL of penicillin, 0.1 mg/mL of streptomycin, 0.25 mg/mL of amphotericin B, and 5% FBS at 37° with 5% CO_2 in a humidified atmosphere.

2.3. cDNA cloning of mCB_2

The plasmid, pUC18-mCB_2, containing the mCB_2 coding sequence was a gift from Dr. T. Bonner (Genetics Section, NIMH). The plasmids pSFV1 and pSFV3-lacZ were from GIBCO-BRL. All plasmids were replicated in DH5α *Escherichia coli* and purified using the Qiagen Mini-Plasmid Kit. The mCB_2 coding sequence was digested from pUC18-mCB_2 with *Bam*HI and *Nco*I, subjected to an end-filling reaction using DNA polymerase I, and cloned into the *Bam*HI site of pSFV1 creating pSFV1-mCB_2.

2.4. Generation of recombinant RNA and receptor expression

The plasmids pSFV1-mCB_2 and pSFV3-lacZ were linearized by digestion with *Spe*I. RNA was generated *in vitro*

from the linearized plasmids using SP6 RNA polymerase. Briefly, linearized plasmid (1.5 μg) was placed in SP6 buffer [0.2 M Tris–HCl (pH 7.9), 30 mM $MgCl_2$, and 10 mM spermidine–$(HCl)_3$], 1 mM m7GpppG RNA capping analog, 1 mM dithiothreitol, NTP mix (final concentration of 1 mM ATP, 1 mM CTP, 1 mM UTP, and 0.5 mM GTP), 50 U ribonuclease inhibitor, and 38 U SP6 RNA polymerase for 4 hr at 37°. For electroporation of recombinant construct RNA, BHK-21 cells at 80–90% confluency were trypsinized with trypsin-EDTA, washed twice with PBS, and resuspended at 1×10^7 cells/mL in PBS. SFV3-lacZ or SFV1-mCB_2 RNA (30 μg) was electroporated into 400 μL of BHK-21 cells at 500 V, 100 μF, and 720 Ω resistance in 2 mM gap BTX disposable cuvettes using the BTX Electro Cell Manipulator 600 (BTX). Cells then were diluted 1/20 with complete G-MEM and added to T-25 cm culture flasks or 60 mm culture dishes for RNA isolation or protein expression analysis, respectively. Potassium chloride (Fisher Scientific) was added at a final concentration of 50 mM to cultures to be used for protein analysis to increase protein production. Cells were harvested at 9–20 hr post-electroporation.

2.5. RNA isolation and northern blot analysis

RNA was isolated from transfected BHK-21 cells by lysis directly in T-25 flasks with 2 mL TRIzol Reagent (GIBCO-BRL) using the instructions of the manufacturer. RNA was separated by agarose gel electrophoresis, transferred overnight in 20× SSC (3 M sodium chloride/0.3 M sodium citrate) onto Nitropure supported nitrocellulose (Micron Separations Inc.), and cross-linked using a Stratagene UV Stratalinker 1800. Membranes were prehybridized (2 hr) in Denhardt's solution [0.1% SDS, 50 mM sodium phosphate, 5× SSC (0.75 M sodium chloride/0.075 M sodium citrate), 0.05 g BSA, 0.05 g Ficoll, 0.05 g polyvinylpyrrolidone, 250 mg yeast RNA, and 50% formamide]. Hybridization solution consisted of prehybridization solution plus radiolabeled mCB_2 cDNA obtained from pUC18-mCB_2. Radiolabeling was performed using the *redi*prime DNA labeling system (Amersham) according to the protocol of the manufacturer. Hybridization was performed overnight at 42°. Membranes then were washed successively in 1× SSC containing 0.2% SDS (42°, 20 min), 0.5× SSC containing 0.2% SDS (42°, 20 min), 0.5× SSC containing 0.2% SDS (55°, 20 min), and 0.1× SSC containing 0.2% SDS (42°, 20 min). Autoradiography was carried out at −80° overnight using XAR imaging film (Eastman Kodak Co).

2.6. Urea-SDS–PAGE and western immunoblotting

Cells were scraped into the culture supernatant, pelleted by centrifugation (4000 *g*, 10 min, 4°), washed with PBS, and resuspended in 100 μL of cold TSA buffer (2 mM Tris–HCl, pH 8.0, 140 mM NaCl, 0.025% sodium azide) and 100 μL of cold TSA buffer containing 2% Triton X-100, 5 mM iodoacetamide, 0.2 U/mL of aprotinin, and 1 mM PMSF. Samples were vortexed and rocked at 4° for 1 hr. Following the addition of 40 μL (0.2 vol.) of 5% sodium deoxycholate (Fisher), samples were incubated on ice for 10 min followed by centrifugation at 4° for 10 min at 4000 *g*. The lysate supernatants were stored in a fresh tube at −80° until examined by urea-SDS–PAGE.

For urea-SDS–PAGE, cell lysates were solubilized (70°, 5 min) (1:1) with 2× sample loading buffer (5% β-mercaptoethanol, 2% SDS, 10% glycerol, 62.5 mM Tris, pH 6.8, 0.2% bromophenol blue, 12 M urea). Proteins were separated by 6 M urea-10% SDS–PAGE on a 1.5-mm thick gel for 4 hr at 30 mA/gel. Following electrophoresis, proteins were transferred overnight at room temperature onto PVDF-Plus membrane (Micron Separations, Inc.) at 90 mA using a Bio-Rad Blot Cell (Bio-Rad Laboratories). The membrane was treated overnight in Blocker Casein in TBS supplemented with 0.05% Tween-20, and incubated (room temperature, 2 hr) with affinity-purified rabbit anti-mCB_2 (CB2-YL) diluted 1:100 in Blocker Casein in TBS supplemented with 0.05% Tween-20. The anti-mCB_2 (CB2-YL) was elicited in rabbits to the mCB_2 peptide encompassing amino acids 320–336 linked chemically to keyhole limpet hemocyanin using procedures described previously [20]. The blot was washed (3 × 15 min each) in TBS, pH 7.4, and incubated (room temperature, 1 hr) with horseradish peroxidase-conjugated goat anti-rabbit IgG (heavy and light chains) (Cappel) diluted 1:25,000 in TBS, pH 7.4, containing Blocker Casein and 0.05% Tween-20. Following washing (6 times, 10 min each) in TBS, pH 7.4, enhanced chemiluminescence was performed using Supersignal CL-HRP (Pierce). The blot was exposed on Kodak XAR imaging film (Eastman Kodak Co) for 1 min.

2.7. [^{35}S] Metabolic protein labeling

Metabolic labeling of transfected BHK-21 cells was performed using [^{35}S]TRAN label (ICN) with a specific activity of 1175 Ci/mmol. Cells were mock-electroporated or electroporated with recombinant SFV1-mCB_2 RNA or SFV3-lacZ RNA and plated into 60 mm dishes. At 8.5 hr following electroporation, the medium was removed and the cultures were maintained for 0.5 hr in methionine-free and cysteine-free DMEM (BioWhittaker). This medium then was replaced with DMEM containing 5% FBS plus 25 μCi/mL of [^{35}S]TRAN label, and cultures were harvested at different time points thereafter. Solubilized protein samples (1×10^6 TCA-precipitable counts) were subjected to 6 M urea-10% SDS–PAGE followed by autoradiography using Kodak XAR imaging film. Autoradiographs of ^{35}S-labeled proteins were exposed to imaging film for 4–5 days.

2.8. Immunofluorescence

Transfected BHK-21 cells were seeded into 6-well plates containing 12 mm circle coverslips (Fisher Scientific)

pre-sterilized under UV light. Coverslips were removed from the tissue culture wells at different time points, washed in PBS, air-dried, fixed (5 min, room temperature) in absolute acetone, and air-dried. For detection of mCB_2, coverslips were rehydrated (2 min) in PBS, blocked (1 hr, room temperature) with Superblock in PBS (Pierce), and incubated (1 hr) with anti-mCB_2 (CB2-YL) diluted 1:10 in Superblock solution. Coverslips then were washed in PBS followed by incubation (1 hr) with FITC-conjugated goat anti-rabbit IgG (1:32 in PBS). Normal rabbit IgG and secondary antibody used alone served as controls. Coverslips were washed in PBS, rinsed in dH_2O, mounted with Aquamount (Lerner Laboratories), and examined on an Olympus BHA microscope equipped with a model BH2RFL reflected fluorescence attachment and a PM-10AD photomicrographic system (Olympus Corp.).

2.9. Treatment of SFV1-mCB_2 RNA-transfected BHK-21 cells with 2-deoxy-D-glucose

BHK-21 cells were mock-transfected or transfected with SFV1-mCB_2 RNA or SFV3-lacZ RNA. Nine hours later, [^{35}S]TRAN label (25 μCi/mL) was added to the cultures in the presence or absence of 2-deoxy-D-glucose (0.1 or 0.2%). Cells were harvested 12 hr later, and whole cell homogenates (10^6 TCA-precipitable counts/well) were subjected to immunoprecipitation using affinity-purified anti-mCB_2 antibody in concert with Protein A sepharose [21]. Briefly, homogenates were brought up to a volume of 200 μL in dilution buffer (0.1% Triton X-100, 0.1% BSA, prepared in TSA buffer) and incubated overnight with a 20-μL suspension of Protein A sepharose beads (Pharmacia Biotech AB) prepared as described by the manufacturer. Samples then were centrifuged (1 min, 4°, 200 *g*), and the supernatants were transferred to new Eppendorf tubes precoated with dilution buffer. To the supernatants 1 μL of anti-CB2-YL was added. Following incubation for 1.5 hr at 4° with rocking, 50 μL of Protein A sepharose was added, and the mixtures were incubated for an additional 1.5 hr with rocking. Samples were centrifuged, the supernatants were discarded, and the pelleted beads were washed twice with 1 mL of dilution buffer, once with TSA solution, and once with stacking gel buffer (0.05 M Tris, pH 6.8). Beads were resuspended in 25 μL of 2× sample loading buffer, the mixture was incubated for 5 min followed by centrifugation (1 min, 200 *g*, 4°), and the supernatant was subjected to 6 M urea-10% SDS–PAGE and autoradiography by exposure to imaging film for 4–5 days.

2.10. Treatment of SFV1-mCB_2 RNA-transfected BHK-21 whole cell homogenates with PNGase F

Mock-transfected or SFV1-mCB_2-transfected BHK-21 cells were subjected to metabolic labeling with [^{35}S]TRAN (25 μCi/mL) and harvested as described above. Cells were solubilized in cold TSA buffer containing 2% Triton X-100 and protease inhibitors (5 mM iodoacetamide, 0.2 U/mL of aprotinin, and 1 mM PMSF). Following incubation (5 min) at room temperature in the presence of 0.1 M β-mercaptoethanol and 0.5% SDS, the protein homogenates (10 μL, 10^6 counts) were mixed with 25 μL of 0.5 M Tris–Cl (pH 8.0), 10 μL of 0.1 M 1,10-phenanthroline, 10 μL of 10% Triton X-100, and 1.5 units of PNGase F and incubated overnight at 30°. Homogenates then were subjected to immunoprecipitation, 6 M urea-10% SDS–PAGE, and autoradiography as described above.

2.11. Radioligand binding

The radioligand binding assay was modified from that reported previously by Compton *et al.* [22]. Mock-transfected and SFV1-mCB_2-transfected BHK-21 cells were harvested at 21 hr post-transfection, washed in PBS, and suspended in Solution I (320 mM sucrose, 50 mM Tris–HCl, 2 mM EDTA, 5 mM $MgCl_2$, pH 7.4). Cells were homogenized and centrifuged (100 *g*, 10 min, 4°), the supernatant was collected, and the pellet was subjected to two additional rounds of homogenization in Solution I and centrifugation. The combined supernatants were centrifuged at 100,000 *g* for 1 hr at 4°, and the pellet was resuspended in Solution II (50 mM Tris–HCl, 1 mM EDTA, 3 mM $MgCl_2$, pH 7.4), divided into aliquots, and stored at −80°. Binding was initiated by the addition of protein to sialinized tubes containing [^{3}H]CP55940 (165 Ci/mmol, Dupont/NEN) in Buffer A (50 mM Tris–HCl, 1 mM EDTA, 3 mM $MgCl_2$, 5 mg/mL of fatty acid free BSA, pH 7.4) to 0.5 mL. Unlabeled CP55940 (1 μM) was used to assess nonspecific binding. Following incubation (30°, 1 hr), binding was terminated by the addition of 2 mL of Buffer B (50 mM Tris–HCl, 1 mg/mL of BSA, pH 7.4). Samples were collected by vacuum filtration through Whatman GF/C filters pretreated (6 hr) with 0.1% polyethyleneimine. Tubes were washed twice with 2 mL of Buffer B, and the washes were filtered. Filters were washed (2 times) with 4 mL of Buffer B, placed in 5 mL of scintillation fluid overnight, shaken for 1 hr, and subjected to liquid scintillation spectrometry.

Cannabinoids were prepared by suspension in Buffer A from a 1 mg/mL ethanolic solution (final concentration of ethanol was not more than 0.4%). Saturation experiments were conducted with seven concentrations of [^{3}H]CP55940 (N = 3) ranging from 50 pM to 5 nM. The B_{max} and K_d values obtained from Scatchard analysis of saturated binding curves were determined by the KELL package of binding analysis programs (Biosoft). Competition assays were conducted with 1 nM [^{3}H]CP55940 and five concentrations of unlabeled displacing ligand. Specific binding was determined by subtracting nonspecific binding from total binding in the absence of competing ligand. The percentage displacement of specific binding was calculated for the amount of radiolabel bound in the presence of unlabeled displacing ligand. Displacement IC_{50} values were determined by linear regression analysis

of log concentration–percent displacement data using the KELL package of binding analysis programs.

3. Results

3.1. Construction of the mCB_2 recombinant SFV plasmid vector

The coding sequence for the mCB_2 cDNA was excised from pUC18-mCB_2 with *Nco*I and *Bam*HI restriction enzymes and ligated into pSFV1 resulting in a construct designated pSFV1-mCB_2 (Fig. 1). The orientation of the mCB_2 insert was confirmed by restriction enzyme mapping (data not shown). The SFV1-mCB_2 vector then was employed to generate SFV1-mCB_2 recombinant viral RNA (SFV1-mCB_2 RNA) for electroporation into BHK-21 cells.

3.2. Northern analysis of mCB_2 RNA generated by recombinant SFV1-mCB_2 RNA

Northern blot analysis was performed to confirm that electroporated linearized recombinant viral RNA was replicated and transcribed *in vivo*. Two transcripts containing the cloned *mCB_2* gene were produced from virus directed RNA synthesis and represented full-length genome and subgenome RNA (Fig. 2). The band at 8 kb resulted from transcription of the full-length recombinant virus RNA genome. The second band at 1.1 kb is consistent in size with that predicted for the *mCB_2* gene in the SFV1 recombinant virus RNA and results from transcription at the subgenomic promoter. CB_2 transcripts were not observed in the lanes containing total RNA from cells transfected with SFV3-lacZ recombinant viral RNA or subjected to "mock" transfection.

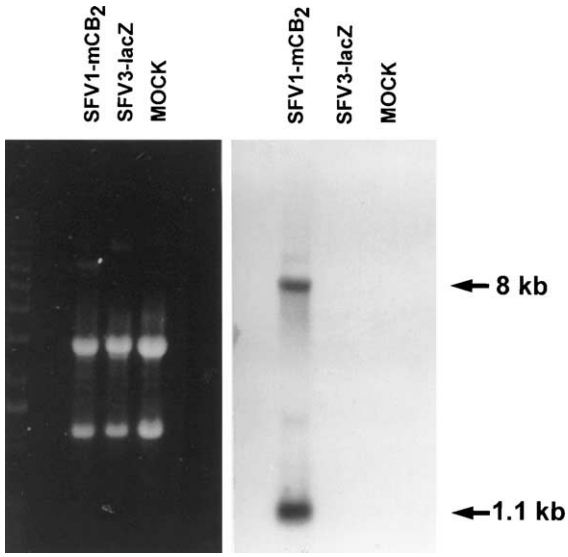

Fig. 2. Northern analysis of transcription from the pSFV1-mCB_2 vector. The plasmid was linearized using an *Spe*I restriction site located after the mCB_2 coding sequence, and SP6 polymerase was used for *in vitro* transcription to yield SFV1-mCB_2 RNA. BHK-21 cells were electroporated with SFV1-mCB_2 RNA or SFV3-lacZ RNA, or were mock-transfected and products of transcription *in vivo* were analyzed. Left panel: total RNA was run on a formaldehyde gel and was stained with ethidium bromide. Right panel: Northern analysis of the total RNA was performed using mCB_2 cDNA as a hybridization probe. Two transcripts were detected in total RNA from SFV1-mCB_2 RNA-transfected cells representing the full-length RNA genome (upper band, 8 kb RNA) and the subgenomic message (lower band, 1.1 kb mRNA).

3.3. Expression of mCB_2 protein

To determine whether novel protein expression occurred in BHK-21 cells transfected with SFV1-mCB_2 RNA which was consistent with that for the mCB_2 receptor, biosynthetic radiolabel incorporation, western immunoblotting, and immunofluorescence experiments were performed.

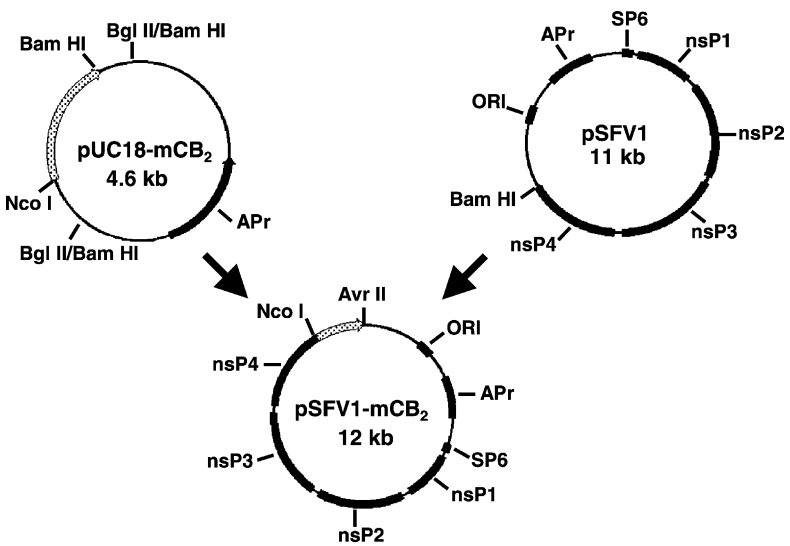

Fig. 1. Construction of the pSFV1-mCB_2 expression vector. The coding sequence for mCB_2 was isolated from pUC18-mCB_2 using *Nco*I and *Bam*HI restriction enzymes and was cloned into the *Bam*HI site of the SFV expression vector pSFV1 resulting in pSFV1-mCB_2.

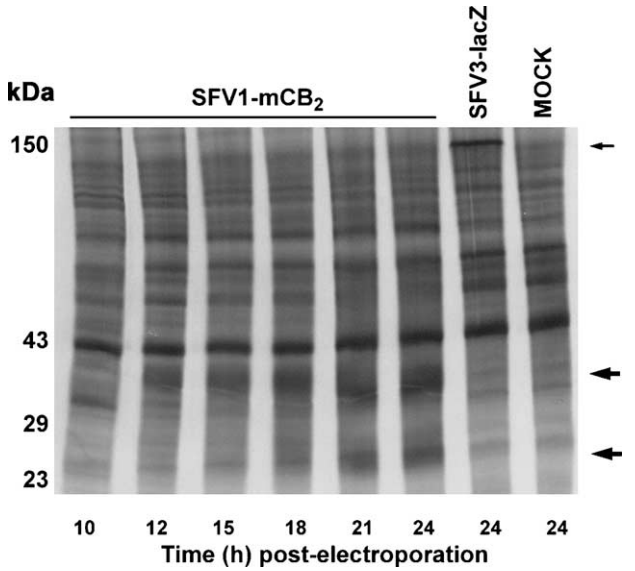

Fig. 3. Time-course expression of mCB_2 protein. Cells were transfected with SFV1-mCB_2 RNA, SFV3-lacZ RNA, or mock-transfected and [^{35}S]TRAN label was added to the cultures 8.5 hr later. Cells were harvested at different time points beginning at 10 hr post-electroporation, and whole cell homogenates were subjected to SDS–PAGE and autoradiography. A time-related accumulation of a novel protein species of approximately 40 kDa (middle arrow) was observed for homogenates from SFV1-mCB_2 RNA-transfected cells. An additional novel protein of 26 kDa (bottom arrow) was observed at late times (i.e. 18 and 24 hr) post-transfection. The small arrow at the top designates the position of the lacZ-specific 115 kDa protein from homogenates of cells transfected with SFV3-lacZ RNA.

Cells were subjected to ''mock'' transfection or to transfection with SFV1-mCB_2 RNA or control SFV3-lacZ RNA. Autoradiographic analysis of homogenates of cells transfected with SFV1-mCB_2 RNA and subjected to radiolabeled amino acid incorporation revealed a time-related accumulation of a novel major protein species of approximately 40 kDa (Fig. 3). Novel protein expression was observed as early as 10 hr post-transfection and reached maximal levels by 24 hr post-transfection. In addition, at a relatively late time period post-transfection (18 and 24 hr post-transfection), an additional novel protein species of approximately 26 kDa was observed. As expected, whole cell homogenates from control SFV3-lacZ RNA-transfected cells exhibited *de novo* accumulation of a 115 kDa product but not of 26 or 40 kDa products. Accumulated levels of protein species of 26, 40, or 115 kDa were not observed for homogenates of ''mock''-transfected cells.

The biosynthetic radiolabel incorporation experiments were complemented with those employing urea-SDS–PAGE and western immunoblotting. Whole cell homogenates of SFV1-mCB_2-transfected cells harvested at 21 hr post-transfection revealed the presence of two major bands of approximately 26 and 40 kDa that were immunoreactive with an affinity-purified anti-mCB_2 antibody (Fig. 4). Immunoreactive species of greater than 40 kDa also were observed but these were at lesser levels. Immunoreactive

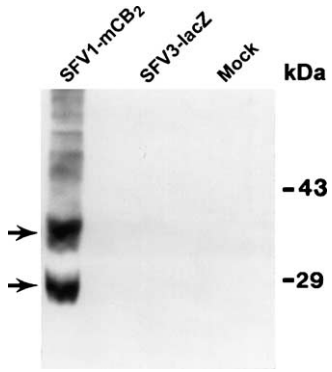

Fig. 4. Western immunoblot of homogenates of BHK-21 cells transfected with SFV1-mCB_2 RNA, SFV3-lacZ RNA, or mock-transfected. Cells were harvested at 21 hr post-transfection, and homogenates were subjected to SDS–PAGE and Western immunoblotting using anti-mCB_2 antibody. Two major immunoreactive bands of approximately 40 and 26 kDa were observed for homogenates from SFV1-mCB_2 transfected cells.

bands were not observed for whole cell homogenates of SFV3-lacZ RNA-transfected or ''mock''-transfected cells.

Immunofluorescence microscopy using anti-mCB_2 antibody revealed intracytoplasmic perinuclear accumulation of immunoreactive product as early as 9 hr post-transfection with SFV1-mCB_2 RNA (Fig. 5A). By 14 hr post-transfection intense immunofluorescence was observed throughout the cytoplasmic compartment (Fig. 5B). At this time period and beyond, the immunoreactive product for mCB_2 was distributed in a reticulated pattern within the cytoplasm consistent with its co-localization with cellular membranes (Fig. 5C).

Immunofluorescence was not detected in cells transfected with SFV3-lacZ RNA or ''mock''-transfected and incubated with anti-mCB_2 antibody (Fig. 5D and E). Similarly, immunofluorescence was not observed for SFV1-mCB_2 RNA-transfected cells incubated with pre-immunization serum derived from the same rabbit that was used to generate the anti-mCB_2 antibody or with anti-mCB_2 preabsorbed with the homologous peptide that was used to generate the anti-mCB_2 antibody.

3.4. Effect of 2-deoxy-D-glucose treatment and PNGase F enzymatic cleavage on mCB_2 expression

To assess whether the mCB_2 expressed in BHK-21 cells was glycosylated at its one potential glycosylation site in the amine terminal extracellular domain, cells were maintained post-transfection in medium containing 2-deoxy-D-glucose, an analog of glucose that results in abortive glycosylation after its incorporation into the sugar chain. Autoradiograms of immunoprecipitates of homogenates of SFV1-mCB_2 RNA-transfected cells treated with 2-deoxy-D-glucose and subjected to biosynthetic radiolabel incorporation and urea-SDS–PAGE revealed accumulation of a smaller species of approximately 38 kDa as compared to the 40 kDa species from cells not treated with 2-deoxy-D-glucose (Fig. 6A). In contrast, no apparent downward

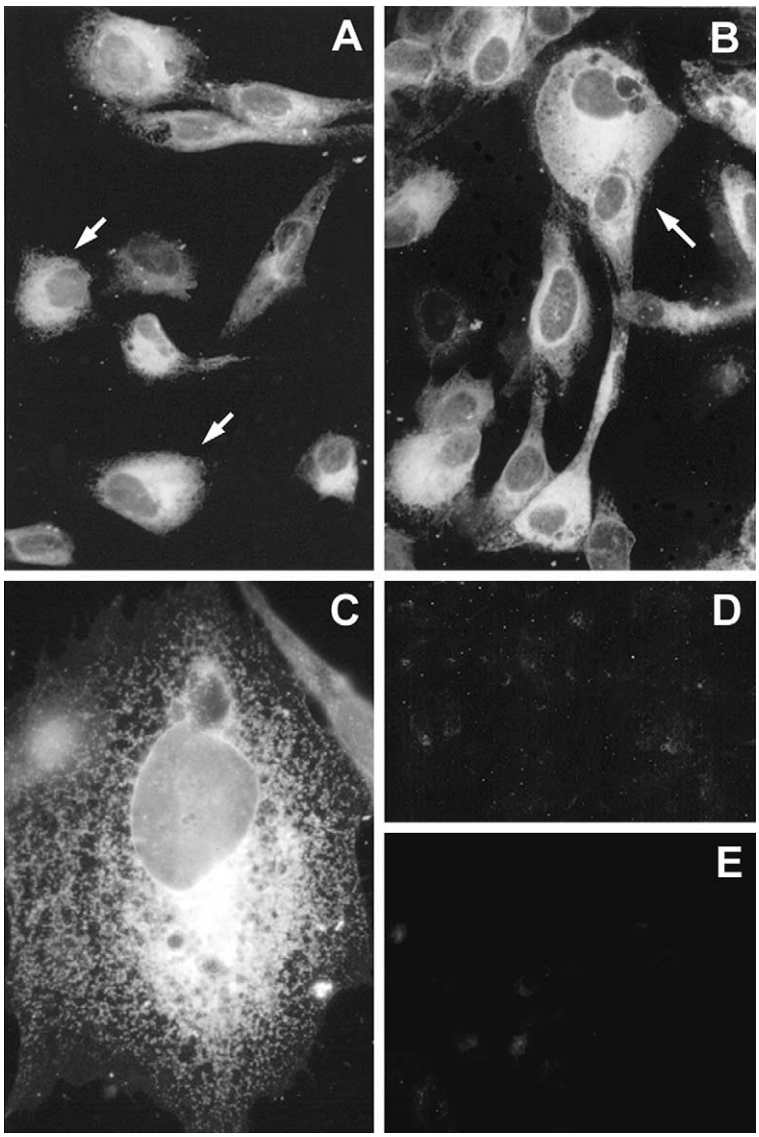

Fig. 5. Immunofluorescence microscopy of cells transfected with SFV1-mCB$_2$ RNA, SFV3-lacZ RNA, or mock-transfected. Cells were treated with affinity-purified rabbit anti-mouse CB$_2$ domain-specific IgG as the primary antibody followed by FITC-conjugated goat anti-rabbit IgG as the secondary antibody. (A) At 9 hr post-transfection, moderate immunofluorescence in a perinuclear "signet ring" pattern was observed in cells transfected with SFV1-mCB$_2$ RNA (arrows). (B) At 14 hr post-transfection, intense immunofluorescence was observed throughout the cytoplasm in cells transfected with SFV1-mCB$_2$ RNA (arrow). (C) Distribution of immunoreactive product in a reticulated pattern for SFV1-mCB$_2$ RNA-transfected cells at 18 hr post-transfection. SFV3-lacZ RNA-transfected (D) and "mock"-transfected (E) cells exhibited minimal fluorescence (A, B, D, and E: 250×; C: 600×).

mobility shift was observed for the 26 kDa species following treatment with 2-deoxy-D-glucose. However, the intensity of this band, as determined by autoradiography, was decreased compared to that of the corresponding band for homogenates of cells not subjected to 2-deoxy-D-glucose treatment.

PNGase F enzymatic treatment, which results in cleavage of the bond between asparagine and *N*-acetylglucosamine and removes the entire sugar residue from protein, indicated the presence of *N*-linked glycosylation for the mCB$_2$ expressed in BHK-21 cells. Immunoprecipitates of homogenates of radiolabeled cells at 21 hr post-transfection treated with PNGase F and subjected to urea-SDS–PAGE revealed depleted levels of the 40 kDa mCB$_2$ species concomitant with accumulation of levels of a species of approximately 38 kDa (Fig. 6B). No apparent effect on the size of the 26 kDa species was noted following PNGase F treatment.

3.5. Characterization of cannabinoid binding to membranes of SFV1-mCB$_2$ RNA-transfected BHK-21 cells

Computer analysis of [^{3}H]CP55940 binding data for cells transfected with SFV1-mCB$_2$ RNA determined a K_d of 0.35 ± 0.04 nM and a B_{max} of 24.4 ± 2.7 pmol/mg. A representative Scatchard–Rosenthal plot for mCB$_2$ radioligand binding is shown in Fig. 7. To identify the pharmacological specificity of the cannabinoid receptors

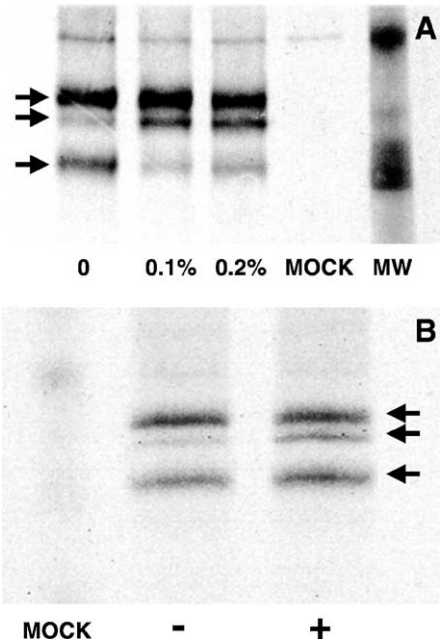

Fig. 6. Effect of 2-deoxy-D-glucose or PNGase F treatment on mCB_2 protein expressed by SFV1-mCB_2 transfected cells. (A) Treatment of SFV1-mCB_2 transfected cells with 2-deoxy-D-glucose. Immunoprecipitates of whole cell homogenates of cells treated with 2-deoxy-D-glucose exhibited accumulation of a smaller (i.e. 38 kDa) species (middle arrow) as compared with similarly transfected cells not treated with 2-deoxy-D-glucose, which expressed the major protein product of 40 kDa (top arrow). Treatment with 2-deoxy-D-glucose had no apparent effect on the size of the 26 kDa product (bottom arrow). The lane designated MW represents the electrophoresed molecular mass standards. (B) Treatment of whole cell homogenates from cells transfected with SFV1-mCB_2 with PNGase F. Cells were radiolabeled and protein lysates were subjected to PNGase F enzymatic digestion, immunoprecipitation, SDS–PAGE, and autoradiography. Immunoprecipitates of whole cell homogenates from cells treated (+) with PNGase F exhibited accumulation of a smaller (38 kDa) gene product (middle arrow) as compared with those not subjected to treatment (−) which contained the major protein product of 40 kDa (top arrow). PNGase F treatment had no apparent effect on the smaller 26 kDa protein species (bottom arrow).

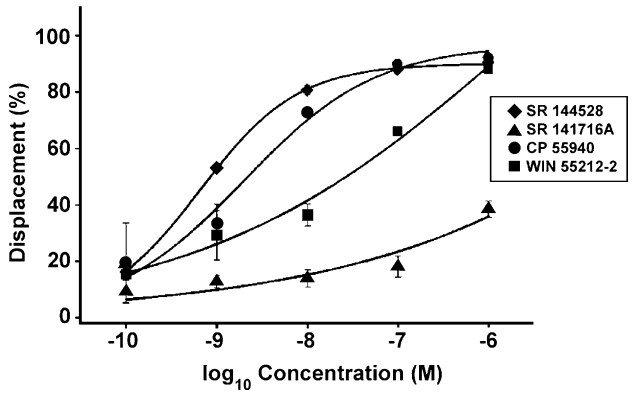

Fig. 8. Displacement of total [^{3}H]CP55940 binding by unlabeled CP55940, WIN55212-2, SR141716A, or SR144528 in membrane preparations of BHK-21 cells transfected with SFV1-mCB_2 recombinant RNA. A rank order of ligand binding was obtained for cells expressing mCB_2 similar to that reported previously for CHO cells [11,24]. Data shown are the means (±SD) of three experiments performed in triplicate.

expressed in BHK-21 cells, binding experiments using unlabeled CP55940, WIN55212-2, SR141716A, and SR144528 to compete with binding of [^{3}H]CP55940 were performed (Fig. 8). Computer analysis indicated IC_{50} values for displacement of specific binding for each compound as follows: SR144528 = 0.66 ± 0.15 nM, CP55940 = 1.4 ± 0.96 nM, WIN55212-2 = 9.6 ± 3.1 nM, and SR141716A = 95 ± 79 μM. The rank order of ligand binding of CP55940 > WIN55212-2 > SR141716A is consistent with that reported previously for mCB_2 expressed in CHO cells and mouse spleen [11,23,25,26]. The expressed receptor was verified as the CB_2 using the CB_2-selective antagonist SR144528, which was able to displace [^{3}H]CP55940 with high affinity, whereas the CB_1-selective antagonist SR141716A could only displace [^{3}H]CP55940 at micromolar concentrations.

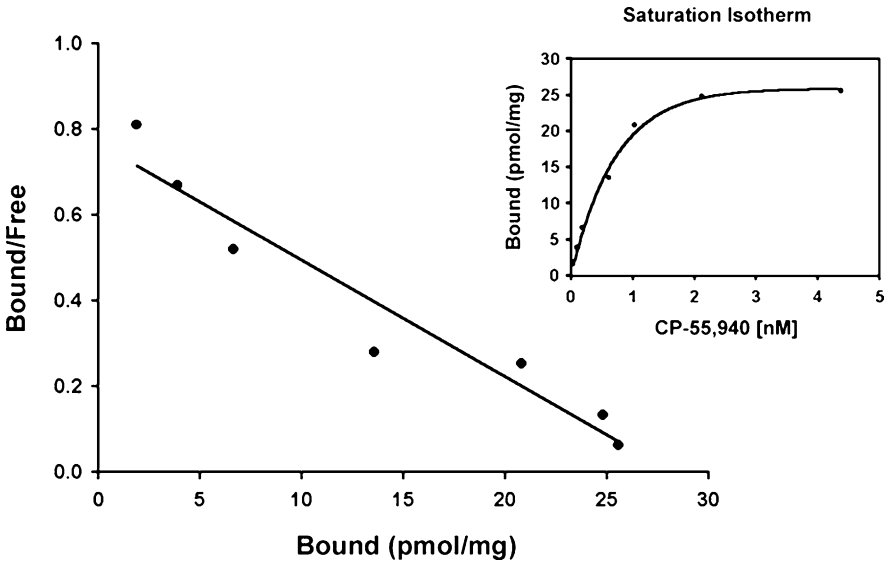

Fig. 7. Scatchard–Rosenthal analysis of [^{3}H]CP55940 receptor binding in membrane preparations of BHK-21 cells transfected with SFV1-mCB_2 recombinant RNA. Inset: saturation isotherm of specific binding from membrane preparations prepared from these cells. The plot indicated a K_d of 0.35 ± 0.04 nM and a B_{max} of 24.4 ± 2.7 pmol/mg. Data points are the means of triplicate determinations.

4. Discussion

In the present study, we report on the application of an SFV construct for the expression of relatively high levels of the mCB_2 in mammalian cells. The CB_1 and CB_2 receptors have been cloned and expressed in *E. coli* and baculovirus-infected insect cells [27,28]. However, while these systems allow for the production of relatively high levels of cannabinoid receptors, post-translational and compartmentation features are restricted to the particular cellular system in which they are expressed and do not represent those native to mammalian cells. Cannabinoid receptors have been expressed in mammalian cells stably transfected with various plasmid vectors [1,3,23,29], but these systems do not allow for the production of preparative levels of receptors. Limitations on the amount of receptor which can be expressed can be overcome using Chinese Hamster Ovary (CHO) cells, but newly expressed protein may not reflect distinctive post-translational and compartmentalization properties of disparate cell types in which the CB_2 is expressed natively. SFV vectors offer the advantage of allowing for expression of protein-encoding sequences in a wide variety of mammalian cell types [30–34]. Receptors can be expressed which incorporate cell-specific glycosylation and protein modifications. In addition, since recombinant SFV RNA generated *in vitro* is of positive polarity, it can be amplified within the cell as a consequence of its self-encoded RNA replicase. The same replicase produces a shorter RNA species encoding the gene product of interest, which generates a high copy number of receptor independently of strictures imposed by nuclear transcriptional factors.

In the present study, transfection of SFV1-mCB_2 RNA into BHK-21 cells resulted in generation of recombinant mCB_2 viral RNA and of message for the mCB_2 as evidenced by the identification of 8 and 1.1 kb RNA species by northern analysis. In addition, production of translational product consistent with that representing the mCB_2 receptor was observed. Time-course experiments, conducted for the monitoring of biosynthetic incorporation of radiolabeled amino acids indicated *de novo* synthesis of a major novel gene product of approximately 40 kDa for cells transfected with SFV1-mCB_2 RNA but not for ''mock''-transfected cells or cells transfected with SFV3-lac Z RNA. This gene product exhibited a time-related augmentation from 10 through 24 hr post-transfection. In addition, a second novel gene product of approximately 26 kDa was observed in whole cell homogenates of cells transfected with SFV1-mCB_2. This smaller product was detected at relatively high levels at 18 and 24 hr post-transfection, time periods that are at a relatively late stage in recombinant SFV gene expression. Western immunoblot analysis indicated that the two gene products were antigenically related, at least in terms of shared domains correlative to that encompassing amino acids 320–336 of the mCB_2. Additional immunoreactive bands of apparent higher molecular mass that were observed were at minor levels and may represent aggregated mCB_2. Such an outcome is not unanticipated since cannabinoid receptors, typical of G protein-coupled receptors, are hydrophobic, and incomplete solubilization may have occurred in spite of treatment of samples with SDS in concert with both β-mercaptoethanol and urea as reducing and chaotropic agents, respectively. An alternative explanation is that the apparent higher molecular mass products represent receptor homodimers and higher oligomers. G protein-coupled receptors have been shown to exist as homo-oligomeric and hetero-oligomeric complexes in living cells. Van Brocklyn *et al*. [35] demonstrated that sphingosine-1-phosphate (S1P) receptors form both homodimers and heterodimers with other members of the S1P subfamily of receptors. Romano *et al*. [36] indicated that metabotropic glutamate receptors exist as covalent dimers. Oligomerization also has been reported for dopamine, seratonin, opioid, and γ-aminobutyric acid (GABA) receptors [37–39]. However, it is important to note that in the present investigation an expression system was employed that resulted in over-production of the mCB_2. Thus, formation of dimers and higher oligomers could be the result of hyper-expression of receptors rather than representing a native configuration. In addition, it is possible that the higher relative molecular mass species were formed during the cellular solubilization process. Studies are in progress to resolve whether higher oligomers exist natively and, if so, to establish their functional relevance. The SDS–PAGE and western immunoblot analyses were complemented with those using the anti-mCB_2 antibody in immunofluorescence microscopy studies. Immunofluorescence analysis confirmed expression of product immunoreactive for mCB_2 following transfection of BHK-21 cells with SFV1-mCB_2 RNA. Immunoreactivity for the mCB_2 was not detected in cells that were ''mock''-transfected or transfected with SFV3-lacZ RNA.

Experiments using 2-deoxy-D-glucose and PNGase F indicated that the 40 kDa receptor species, but not the 26 kDa species, which was expressed in BHK-21 cells transfected with SFV1-mCB_2 RNA, was glycosylated. 2-Deoxy-D-glucose was employed in these studies since it is a structural analog of mannose and induces inhibitory effects on glycoprotein synthesis as a result of direct incorporation into the carbohydrate moiety [40]. Once incorporated into the elongating oligosaccharide side chain of glycoprotein in place of mannose, glycosyl transferases apparently do not recognize the deoxy-sugar and glycosylation is terminated prematurely [41,42]. Premature termination of glycosylation results in the production of a glycoprotein with incomplete oligosaccharide side chains which is recognized as a protein species exhibiting a downward mobility shift upon SDS–PAGE when compared with the same glycoprotein produced by cells not treated with 2-deoxy-D-glucose. In the present study, SFV1-mCB_2 RNA-transfected BHK-21 cells maintained in the presence

of 2-deoxy-D-glucose generated a smaller protein species of approximately 38 kDa as compared with cells similarly transfected but not treated with 2-deoxy-D-glucose. In contrast, no downward mobility shift was observed for the 26 kDa product generated for SFV1-mCB_2 RNA-transfected cells treated with 2-deoxy-D-glucose consistent with the absence of a glycosylated moiety for this smaller species.

The 2-deoxy-D-glucose experiments were complemented with those in which the expressed mCB_2 protein was subjected to cleavage by PNGase F. PNGase F cleaves the sugar moiety from glycoprotein at the asparagine-sugar bond and indicates the presence of *N*-linked glycosylation [43]. As in the case for 2-deoxy-D-glucose treatment, digested glycosylated protein can be identified as a species exhibiting a downward mobility shift upon SDS–PAGE when compared with the undigested protein.

Immunoprecipitates of protein lysates obtained from radiolabeled cells transfected with SFV1-mCB_2 RNA and incubated with PNGase F yielded a protein species that exhibited a downward mobility shift upon SDS–PAGE. In agreement with the 2-deoxy-D-glucose data, no apparent effect on the size of the 26 kDa species was observed following PNGase F treatment. However, a distinctive difference between 2-deoxy-D-glucose and the PNGase F experiments was that relatively lower amounts of the 26 kDa species were observed for immunoprecipitates of whole cell homogenates of cells treated with 2-deoxy-D-glucose as compared with similarly transfected cells not treated with 2-deoxy-D-glucose. PNGase F treatment, on the other hand, had no apparent effect on levels of the smaller 26 kDa protein species. These observations suggest that the apparent lower amounts of the 26 kDa species for cells treated with 2-deoxy-D-glucose were due to effects of the glucose analog itself rather than to inherent properties of less stability or shorter half-life for the protein. However, the mode by which 2-deoxy-D-glucose treatment results in these apparent lower levels has not been determined. Collectively, the 2-deoxy-D-glucose and PNGase F experiments indicate that the 40 kDa mCB_2 receptor species expressed by SFV1-mCB_2 RNA-transfected cells is glycosylated and has a sugar moiety which is *N*-linked to the protein ''backbone'' and contains mannose residues. The occurrence of glycosylation for the larger species is consistent with that anticipated for the native mCB_2 based on the presence of one potential glycosylation site at the amino acid 11 position in the extracellular amine terminal domain of the receptor [11]. In contrast, the smaller species, although sharing immunoreactivity with the larger species, apparently does not contain this glycosylation moiety.

The collective data obtained through biosynthetic radiolabel incorporation for assessment of *de novo* protein expression, immunocytochemistry utilizing affinity-purified and mCB_2 domain-specific antibody, and glycosylation truncation analysis indicate that the 40 kDa protein produced by SFV1-mCB_2 RNA-transfected cells represents native mCB_2. Indeed, the size of the 40 kDa species, as determined through radiolabel incorporation and western immunoblotting experiments, approximates that predicted for the mCB_2 receptor based on extrapolation of its cDNA coding sequence, which yields a molecular mass of 38.2 kDa for post-translationally unmodified receptor [11]. The 26 kDa gene product, on the other hand, may represent product generated from an alternative translational start site from the mCB_2 transcript produced by the transfected SFV1-mCB_2 RNA. The absence of multiple immunoreactive bands smaller than 26 kDa as visualized by western immunoblotting suggests that this smaller species does not represent a product of proteolytic degradation. Also, the smaller species is apparently not a result of translation from an alternative transcription splice variant since it was recombinant viral RNA that was transfected into cells and only the RNA species of 8 and 1.1 kb were observed by northern analysis. In addition, the affinity-purified anti-mCB_2 antibody that was employed in western analyses was elicited to a peptide corresponding to amino acids 320–336, a peptide domain that is localized at the intracellular carboxyl terminal domain of the mCB_2 [11]. Furthermore, extrapolation of the coding sequence for the mCB_2 indicates the presence of an internal methionine residue at amino acid position 115. If the cognate codon were utilized as an alternative translational start site, it would result in the expression of a protein product of approximately 26 kDa. Such a product would retain the peptide domain encompassing amino acids 320–336 and thus exhibit immunoreactivity to the anti-mCB_2 (CB2-YL) antibody.

Eukaryotic mRNAs have been reported to produce more than one protein through alternative translational initiation (ATI) at different AUG codons. Vittorioso *et al.* [44] indicated the occurrence of multiple translational start sites on the mRNA of the albino-3 (*al-3*) gene of *Neurospora crassa*, which encodes the carotenoid biosynthetic enzyme geranylgeranyl-pyrophosphate synthase. In their experiments, molecular analysis of an *al-3* mutant carrying a deletion within the coding sequence revealed that a fraction of ribosomes initiated protein synthesis from either of two internal in-frame AUG codons located downstream of the deletion. Furthermore, the protein product derivative of translation from these downstream AUG codons, although shortened, retained geranylgeranyl-pyrophosphate synthase activity. Wolfe *et al.* [45] performed functional analysis of multiple AUG codons in the transcripts of the STA2 glucoamylase gene of *Saccharomyces cerevisiae*. It was demonstrated that utilization of alternative translational start sites resulted in glucoamylases that differed in N-termini and patterns of localization. Xiong *et al.* [46] reported on regulation of CCAAT/enhancer-binding protein-β (C/EBPβ) isoform synthesis in COS-1 cells through ATI at multiple AUG start sites. These investigators proposed that formation of C/EBPβ isoforms occurred by a ''leaky'' ribosomal scanning mechanism that facilitates ATI of multiple internal AUGs. Thus, there is a precedence

for translation from alternative start sites and a similar mechanism may be operative for recombinant mCB_2 expression using the SFV1-mCB_2 RNA vector. In this context, it is possible that the smaller 26 kDa mCB_2 species may be the translational outcome of ''leaky'' ribosomal scanning inherent in an expression system characterized by high level output of recombinant protein. Whether there is a biological relevance for alternative translation from AUG1 and AUG2 start sites for CB_2 transcripts has not been resolved due to the paucity of biochemical and immunochemical studies that have been performed related to protein expression of native CB_2 receptors. Galiègue *et al*. [7] have indicated that, although gene expression for CB_2 receptors in immune cells is at relatively low levels as compared to that for CB_1 receptors in the brain, there is an ordered profile for amounts of CB_2 mRNAs with natural killer (NK) cells and B lymphocytes expressing highest levels vs. other immune cell types. Thus, studies using NK cells and B lymphocytes for assessment of expression of CB_2 receptors as protein entities may allow for resolution of this issue.

Finally, the recombinant mCB_2 that was expressed in BHK-21 cells exhibited a cannabinoid ligand binding profile consistent with that for the native mCB_2. Specific binding of [^{3}H]CP55940 was obtained for P2 membrane preparations for mCB_2 receptor-expressing cells, while no specific binding was recorded for membranes of uninfected BHK-21 cells or cells transfected with SFV3-lacZ RNA. The association of ligand binding with P2 membrane preparations is consistent with CB_2 receptors as appropriately compartmentalized within cellular membranes. The resulting Scatchard plots indicated a K_d of 0.35 ± 0.04 nM and a B_{max} of 24.4 ± 2.7 pmol/mg. The presence of high amounts (B_{max} of 24.4 ± 2.7 pmol/mg) of binding sites indicated the high level of over-expression of mCB_2 especially when compared to the level of CB_2 expression reported for cells from the human myelomonocytic cell line U937 (525 fmol/mg) or when expressed in a baculovirus expression system (5.24 pmol/mg) [6,28]. These receptors were confirmed as being of the CB_2 receptor type since the CB_2 receptor-specific antagonist SR144528, but not the CB_1 specific antagonist SR141716A, was able to displace [^{3}H]CP55940 at sub-micromolar concentrations. Furthermore, the integrity of the binding sites of the mCB_2 receptor expressed in BHK-21 cells was maintained as cannabinoid binding experiments revealed a rank order of affinities which paralleled that reported previously for the native CB_2 receptor [11,23,24].

In summary, a recombinant SFV construct was employed to express the mCB_2. Relatively high levels of the receptor were produced that were glycosylated, compartmentalized within cellular membranes, and exhibited a cannabinoid ligand binding profile comparable to that reported for the natively expressed mCB_2. These results indicate that SFV systems may serve as valuable *in vitro* models for high-level expression of cannabinoid receptors which retain post-translational and compartmentalization properties native to mammalian cells. Furthermore, because this system allows for high-level expression of ''native'' receptors, it may be possible to apply standard non-denaturation biochemical and/or immunobiochemical procedures for isolation of receptors that retain ligand binding properties. For example, immunoaffinity chromatographic or immunoprecipitation methods using antibodies to amine terminal and extracellular loop domains of the CB_2 could be applied. In addition, as demonstrated in the present study, receptors may be isolated as membrane preparations so that the conformational context of membrane integration and interaction with G proteins is maintained. Such membrane preparations from distinct cell types could allow for the conduct of binding studies under conditions that retain high-affinity binding. In addition, availability of preparative levels of ''natively'' expressed CB_2 receptors would allow for the conduct of studies pursuant to their structural analysis as protein entities and for mapping of the ligand binding in the context of the protein itself. Such studies would provide valuable insight into the design and development of cannabinoid analogs with immune modulating therapeutic potential as well as basic information regarding the functional relevance of CB_2 receptors.

Acknowledgments

This work was supported by National Institutes of Health/NIDA awards DA05832, DA15608 and DA05274.

References

[1] Felder CC, Veluz JS, Williams HL, Briley EM, Matsuda LA. Cannabinoid agonists stimulate both receptor- and non-receptor-mediated signal transduction pathways in cells transfected with and expressing cannabinoid receptor clones. Mol Pharmacol 1992;42:838–45.
[2] Herkenham M, Lynn AB, Little MD, Johnson MR, Melvin LS, de Costa BR, Rice KC. Cannabinoid receptor localization in brain. Proc Natl Acad Sci USA 1990;87:1932–6.
[3] Matsuda LA, Lolait SJ, Brownstein MJ, Young AC, Bonner TI. Structure of a cannabinoid receptor and functional expression of the cloned cDNA. Nature 1990;346:561–4.
[4] Gerard CM, Mollereau C, Vassart G, Parmentier M. Molecular cloning of a human cannabinoid receptor which is also expressed in testis. Biochem J 1991;279(Pt 1):129–34.
[5] Kaminski NE, Abood ME, Kessler FK, Martin BR, Schatz AR. Identification of a functionally relevant cannabinoid receptor on mouse spleen cells that is involved in cannabinoid-mediated immune modulation. Mol Pharmacol 1992;42:736–42.
[6] Bouaboula M, Rinaldi M, Carayon P, Carillon C, Delpech B, Shire D, Le Fur G, Casellas P. Cannabinoid-receptor expression in human leukocytes. Eur J Biochem 1993;214:173–80.
[7] Galiègue S, Mary S, Marchand J, Dussossoy D, Carrière D, Carayon P, Bouaboula M, Shire D, Le Fur G, Casellas P. Expression of central and peripheral cannabinoid receptors in human immune tissues and leukocyte subpopulations. Eur J Biochem 1995;232:54–61.
[8] Munro S, Thomas KL, Abu-Shaar M. Molecular characterization of a peripheral receptor for cannabinoids. Nature 1993;365:61–5.

[9] Buckley NE, Hansson S, Harta G, Mezey E. Expression of the CB_1 and CB_2 receptor messenger RNAs during embryonic development in the rat. Neuroscience 1998;82:1131–49.
[10] Lu Q, Straiker A, Lu Q, Maguire G. Expression of CB_2 cannabinoid receptor mRNA in adult rat retina. Vis Neurosci 2000;17:91–5.
[11] Shire D, Calandra B, Rinaldi-Carmona M, Oustric D, Pessegue B, Bonnin-Cabanne O, Le Fur G, Caput D, Ferrara P. Molecular cloning, expression and function of the murine CB_2 peripheral cannabinoid receptor. Biochim Biophys Acta 1996;1307:132–6.
[12] Griffin G, Tao Q, Abood ME. Cloning and pharmacological characterization of the rat CB_2 cannabinoid receptor. J Pharmacol Exp Ther 2000;292:886–94.
[13] Valk P, Verbakel S, Vankan Y, Hol S, Mancham S, Ploemacher R, Mayen A, Lowenberg B, Delwel R. Anandamide, a natural ligand for the peripheral cannabinoid receptor is a novel synergistic growth factor for hematopoietic cells. Blood 1997;90:1448–57.
[14] Cabral GA, Dove Pettit DA. Drugs and immunity: cannabinoids and their role in decreased resistance to infectious disease. J Neuroimmunol 1998;83:116–23.
[15] Klein TW, Newton C, Friedman H. Cannabinoid receptors and immunity. Immunol Today 1998;19:373–81.
[16] Carayon P, Marchand J, Dussossoy D, Derocq JM, Jbilo O, Bord A, Bouaboula M, Galiègue S, Mondière P, Pénarier G, Le Fur G, Defrance T, Casellas P. Modulation and functional involvement of CB_2 peripheral cannabinoid receptors during B-cell differentiation. Blood 1998;92:3605–15.
[17] McCoy KL, Matveyeva M, Carlisle SJ, Cabral GA. Cannabinoid inhibition of the processing of intact lysozyme by macrophages: evidence for CB_2 receptor participation. J Pharmacol Exp Ther 1999;289:1620–5.
[18] Zhu LX, Sharma S, Stolina M, Gardner B, Roth MD, Tashkin DP, Dubinett SM. Δ-9-Tetrahydrocannabinol inhibits antitumor immunity by a CB_2 receptor-mediated, cytokine-dependent pathway. J Immunol 2000;165:373–80.
[19] Sacerdote P, Massi P, Panerai AE, Parolaro D. In vivo and in vitro treatment with the synthetic cannabinoid CP55,940 decreases the in vitro migration of macrophages in the rat: involvement of both CB_1 and CB_2 receptors. J Neuroimmunol 2000;109:155–63.
[20] Pettit DA, Harrison MP, Olson JM, Spencer RF, Cabral GA. Immunohistochemical localization of the neural cannabinoid receptor in rat brain. J Neurosci Res 1998;51:391–402.
[21] Bonifacino JS, Dell'Angelica EC, Springer TA. Immunoprecipitation. In: Coligan JE, Kruisbeek AM, Margulis DH, Shevad EM, Strober W, editors. Current protocols in immunology. New York: John Wiley; 2001. p. 8.3.1–28.
[22] Compton DR, Rice KC, de Costa BR, Razdan RK, Melvin LS, Johnson MR, Martin BR. Cannabinoid structure–activity relationships: correlation of receptor binding and *in vivo* activities. J Pharmacol Exp Ther 1993;265:218–26.
[23] Showalter VM, Compton DR, Martin BR, Abood ME. Evaluation of binding in a transfected cell line expressing a peripheral cannabinoid receptor (CB_2): identification of cannabinoid receptor subtype selective ligands. J Pharmacol Exp Ther 1996;278:989–99.
[24] Rinaldi-Carmona M, Barth F, Millan J, Derocq JM, Casellas P, Congy C, Oustric D, Sarran M, Bouaboula M, Calandra B, Portier M, Shire D, Breliere JC, Le Fur GL. SR 144528, the first potent and selective antagonist of the CB_2 cannabinoid receptor. J Pharmacol Exp Ther 1998;284:644–50.
[25] Felder CC, Joyce KE, Briley EM, Mansouri J, Mackie K, Blond O, Lai Y, Ma AL, Mitchell RL. Comparison of the pharmacology and signal transduction of the human cannabinoid CB_1 and CB_2 receptors. Mol Pharmacol 1995;48:443–50.
[26] Schatz AR, Lee M, Condie RB, Pulaski JT, Kaminski NE. Cannabinoid receptors CB_1 and CB_2: a characterization of expression and adenylate cyclase modulation within the immune system. Toxicol Appl Pharmacol 1997;142:278–87.
[27] Pettit DA, Showalter VM, Abood ME, Cabral GA. Expression of a cannabinoid receptor in baculovirus-infected insect cells. Biochem Pharmacol 1994;48:1231–43.
[28] Nowell KW, Pettit DA, Cabral WA, Zimmerman Jr HW, Abood ME, Cabral GA. High-level expression of the human CB_2 cannabinoid receptor using a baculovirus system. Biochem Pharmacol 1998;55:1893–905.
[29] Bouaboula M, Bianchini L, McKenzie FR, Pouyssegur J, Casellas P. Cannabinoid receptor CB_1 activates the Na^+/H^+ exchanger NHE-1 isoform via G_i-mediated mitogen activated protein kinase signaling transduction pathways. FEBS Lett 1999;449:61–5.
[30] Szekely L, Jin P, Jiang WQ, Rosén A, Wiman KG, Klein G, Ringertz N. Position-dependent nuclear accumulation of the retinoblastoma (RB) protein during in vitro myogenesis. J Cell Physiol 1993;155:313–22.
[31] Olkkonen VM, Liljestrom P, Garoff H, Simons K, Dotti CG. Expression of heterologous proteins in cultured rat hippocampal neurons using the Semliki Forest virus vector. J Neurosci Res 1993;35:445–51.
[32] Kehm E, Goksu MA, Knopf CW. Expression analysis of recombinant herpes simplex virus type 1 DNase. Virus Genes 1998;17:129–38.
[33] Pettigrew MM, O'Neill SL. Semliki Forest virus as an expression vector in insect cell lines. Insect Mol Biol 1999;8:409–14.
[34] Reddy JR, Kwang J, Varthakavi V, Lechtenberg KF, Minocha HC. Semliki Forest virus vector carrying the bovine viral diarrhea virus NS3 (p80) cDNA induced immune responses in mice and expressed BVDV protein in mammalian cells. Comp Immunol Microbiol Infect Dis 1999;22:231–46.
[35] Van Brocklyn JR, Behbahani B, Lee NH. Homodimerization and heterodimerization of S1P/EDG sphingo-1-phosphate receptors. Biochim Biophys Acta 2002;1582:89–93.
[36] Romano C, Miller JK, Hyrc K, Dikranian S, Mennerick S, Takeuchi Y, Goldberg MP, O'Malley KL. Covalent and noncovalent interactions mediate metabotropic glutamate receptor mGlu5 dimerization. Mol Pharmacol 2001;59:46–53.
[37] Lee SP, Xie Z, Varghese G, Nguyen T, O'Dowd BF, George SR. Oligomerization of dopamine and serotonin receptors. Neuropsychopharmacology 2000;23:S32–40.
[38] George SR, Fan T, Xie Z, Tse R, Tam V, Varghese G, O'Dowd BF. Oligomerization of μ- and δ-opioid receptors. Generation of novel functional properties. J Biol Chem 2000;275:26128–35.
[39] Jones KA, Borowsky B, Tamm JA, Craig DA, Durkin MM, Dai M, Yao WJ, Johnson M, Gunwaldsen C, Huang LY, Tang C, Shen Q, Salon JA, Morse K, Laz T, Smith KE, Nagarathnam D, Noble SA, Branchek TA, Gerald C. $GABA_B$ receptors function as a heteromeric assembly of the subunits $GABA_BR1$ and $GABA_BR2$. Nature 1998;396:674–9.
[40] Steiner S, Courtney RJ, Melnick JL. Incorporation of 2-deoxy-D-glucose into glucoproteins of normal and Simian virus 40-transformed hamster cells. Cancer Res 1973;33:2402–7.
[41] Courtney RJ. Herpes simplex virus protein synthesis in the presence of 2-deoxy-D-glucose. Virology 1976;73:286–94.
[42] Kaluza G, Schmidt MF, Scholtissek C. Effect of 2-deoxy-D-glucose on the multiplication of Semliki Forest virus and the reversal of the block by mannose. Virology 1973;54:179–89.
[43] Freeze HH, Ichikawa M. Identification of *N*-acetylglucosamine-α-1-phosphate transferase activity in *Dictyostelium discoideum*: an enzyme that initiates phosphoglycosylation. Biochem Biophys Res Commun 1995;208:384–9.
[44] Vittorioso P, Carattoli A, Londei P, Macino G. Internal translational initiation in the mRNA from the *Neurospora crassa* albino-3 gene. J Biol Chem 1994;269:26650–4.
[45] Wolfe CL, Lou YC, Hopper AK, Martin NC. Interplay of heterogeneous transcriptional start sites and translational selection of AUGs dictate the production of mitochondrial and cytosolic/nuclear tRNA nucleotidyltransferase from the same gene in yeast. J Biol Chem 1994;269:13361–6.
[46] Xiong W, Hsieh CC, Kurtz AJ, Rabek JP, Papaconstantinou J. Regulation of CCAAT/enhancer-binding protein-β isoform synthesis by alternative translational initiation at multiple AUG start sites. Nucleic Acids Res 2001;29:3087–98.